

Supporting Information

Macroscopic Aerogels with Retained Nanoscopic Plasmonic Properties

Torben Kodanek, Axel Freytag, Anja Schlosser, Suraj Naskar, Thomas Härtling, Dirk Dorfs* and Nadja C. Bigall*

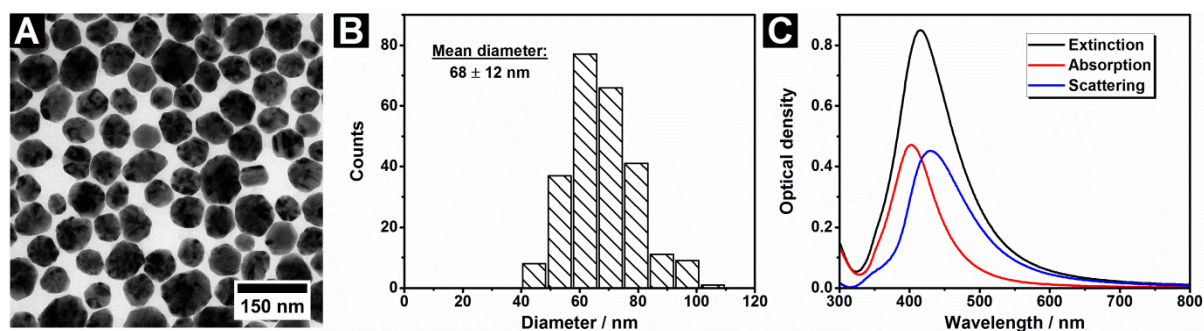


Figure S1. TEM image (A), particle size distribution (B), and UV-vis spectra of the colloidal Ag nanocrystals. In the UV-vis spectra, the resonant scattering (blue curve) was calculated by the subtraction of the absorption (red curve) from the extinction (black curve).

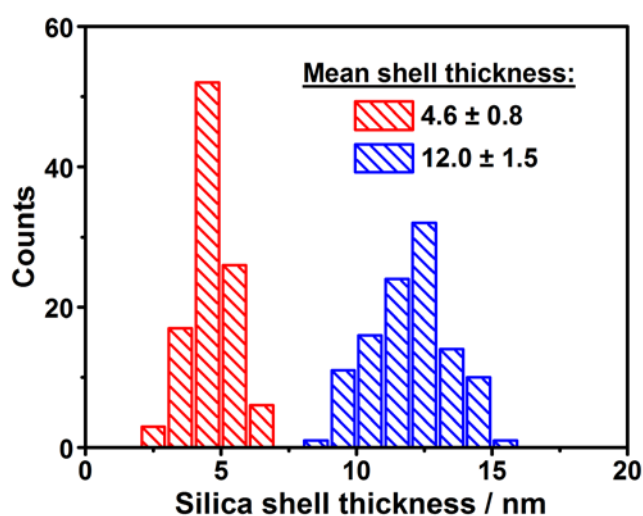


Figure S2. Shell thickness distribution of two different samples of colloidal Ag-SiO₂ core-shell heterostructures obtained by the addition of 20 μ L (red) and 80 μ L (blue) TEOS. The silica shell thickness was determined on the basis of TEM images.

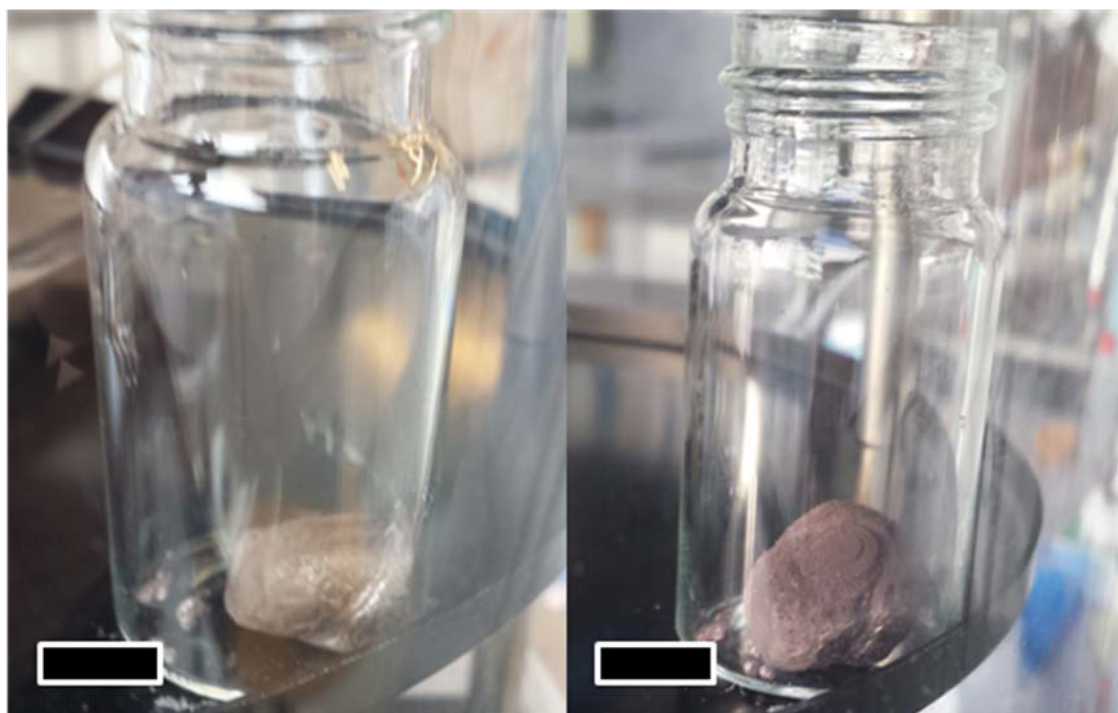


Figure S3. Synthesis of a pure Ag nanocrystal cryoaerogel. 1 mL of a concentrated Ag NP solution ($c_{\text{Ag}} = 29 \text{ mg mL}^{-1}$) were frozen with liquid nitrogen and a photo was taken 15 min after the start of the freeze drying (left image) and after 24h (right image, the monolith rotated around 60° during drying). The mass of the monolith was measured to be 34 mg. The weight difference between solution and monolith is attributed to the uncertainty of measurements, residual PVP ligands (which could not be washed off), and residual water because of the humidity at ambient conditions. Due to no shrinkage a density of 0.03 g cm^{-1} was estimated. The stability of the cryoaerogels does not allow a direct measurement of the density via e.g. flotation measurement.

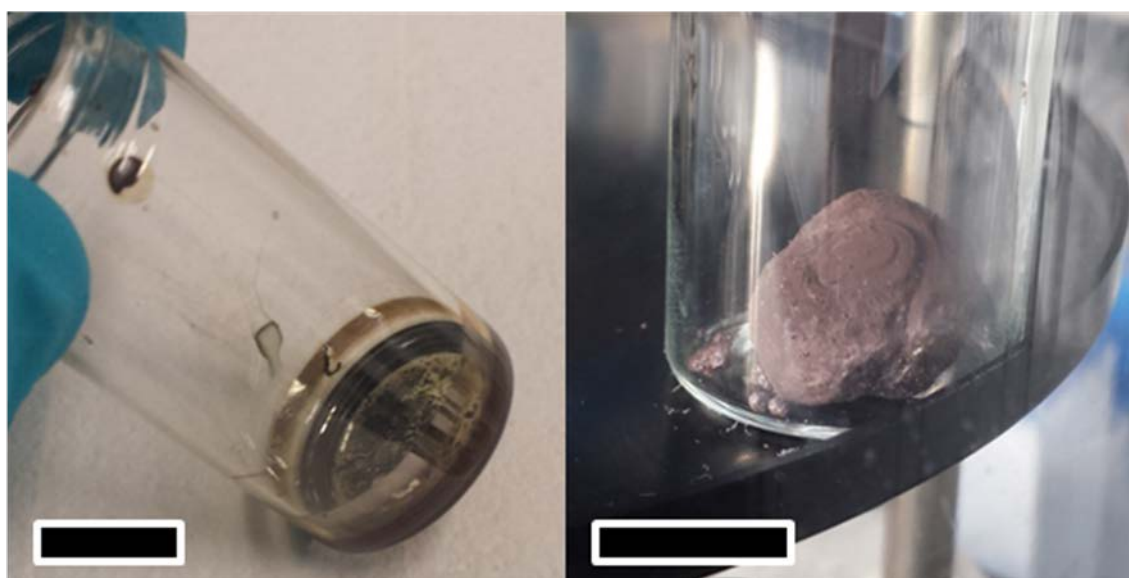


Figure S4. Drying of 1 mL concentrated Ag NP solution ($c_{\text{Ag}} = 29 \text{ mg mL}^{-1}$) after freezing at room temperature (left image) or via freeze drying (right image). The black bar represents 1 cm.

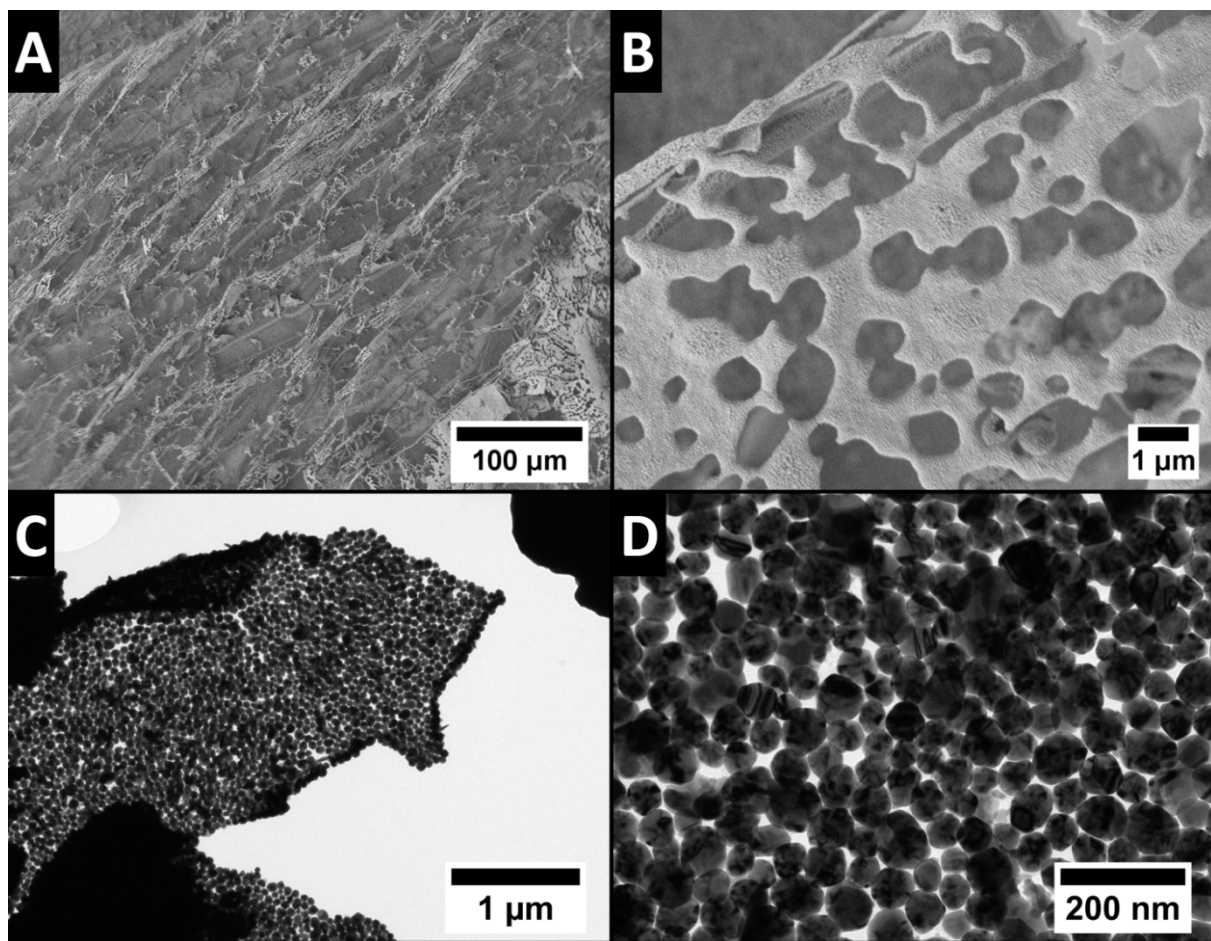


Figure S5. SEM (A+B) and TEM (C+D) characterizations of pure Ag nanoparticles assembled into micrometer thick aerogel films. It can be seen, that the sheets are oriented perpendicular to the substrate, while the nanoparticle are in close proximity.

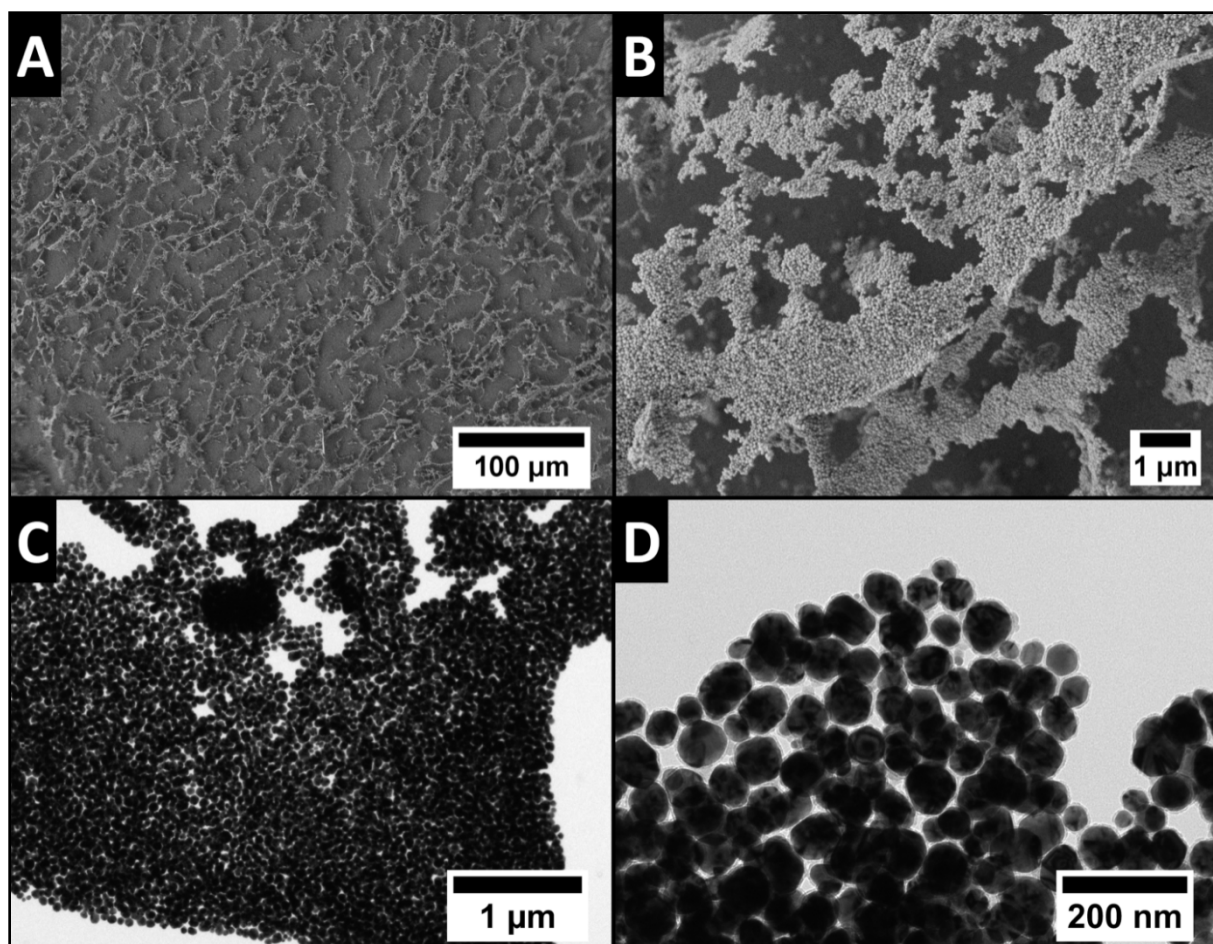


Figure S6. SEM (A+B) and TEM (C+D) characterizations of Ag nanoparticles with a 5 nm silica shell assembled into micrometer thick aerogel films. It can be seen that the sheets are preferably oriented perpendicular to the substrate, while the nanoparticles have a distance of around 10 nm.

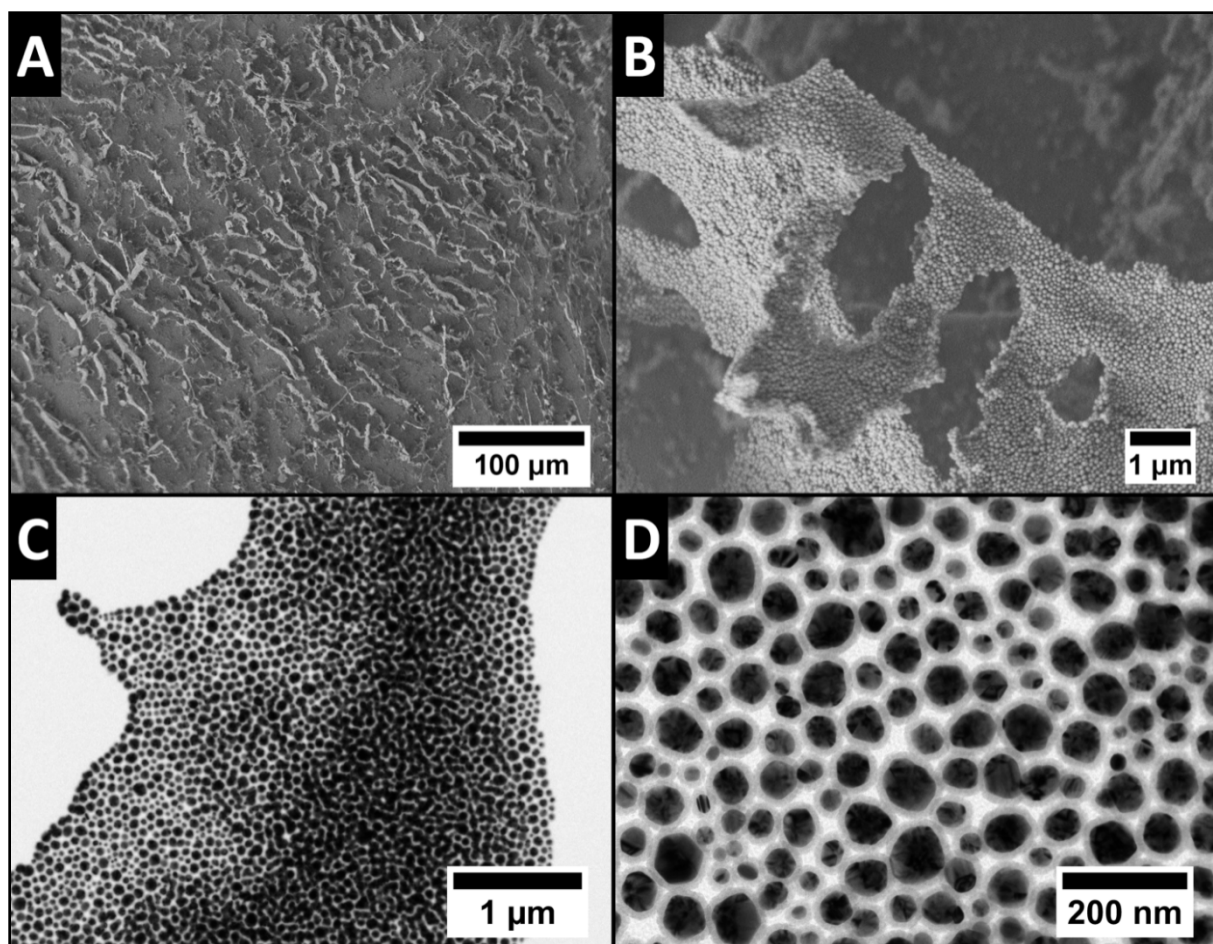


Figure S7. SEM (A+B) and TEM (C+D) characterizations of Ag nanoparticles with a 12 nm silica shell assembled into micrometer thick aerogel films. It can be seen that the sheets are preferably oriented perpendicularly to the substrate, while the nanoparticles have a distance of around 24 nm.

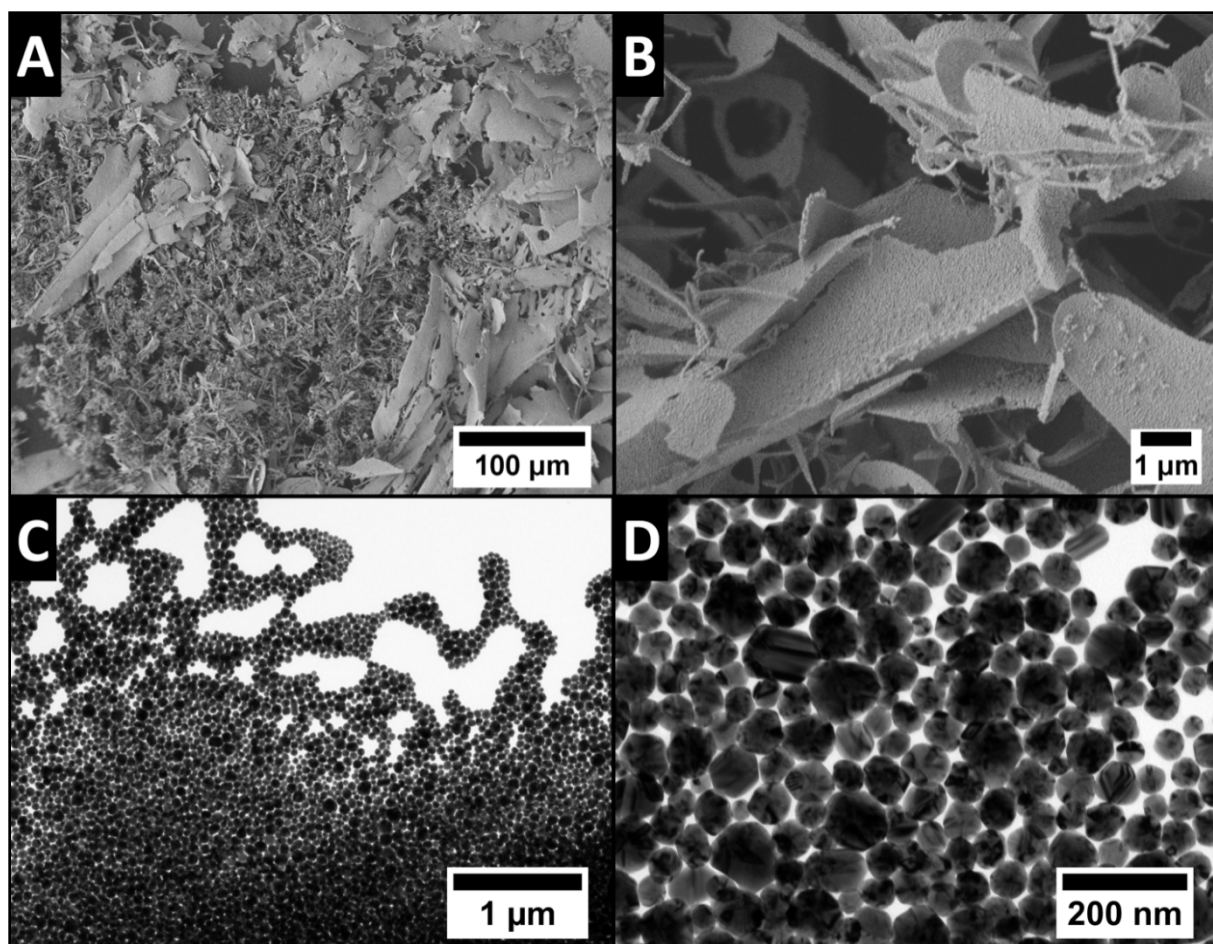


Figure S8. SEM (A+B) and TEM (C+D) characterizations of pure Ag nanoparticles assembled into macroscopic, porous monolithic aerogels. The nanoparticles are in close proximity.

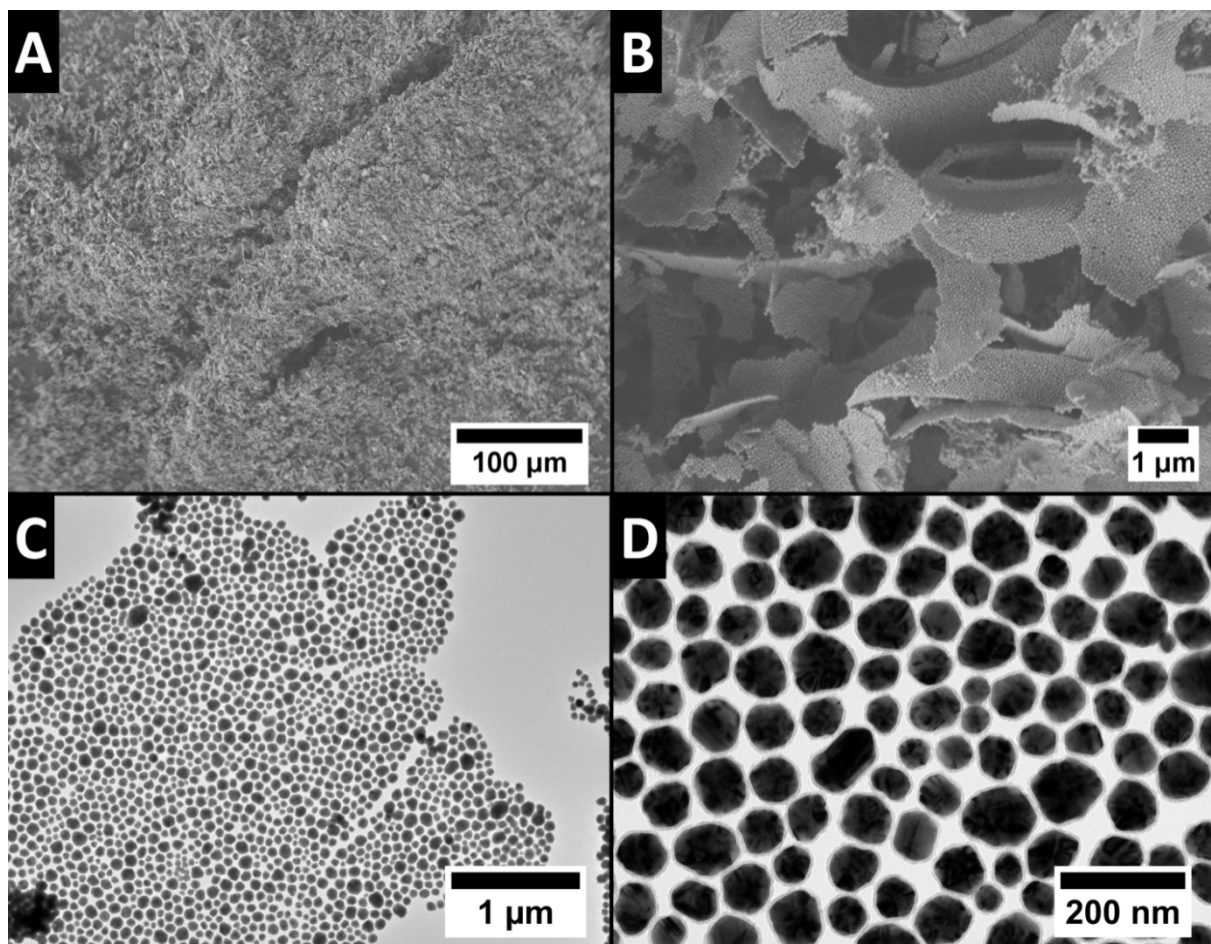


Figure S9. SEM (A+B) and TEM (C+D) characterizations of Ag nanoparticles with a 5 nm silica shell assembled into macroscopic, porous monolithic aerogels. The nanoparticles have interparticle distances of around 10 nm.

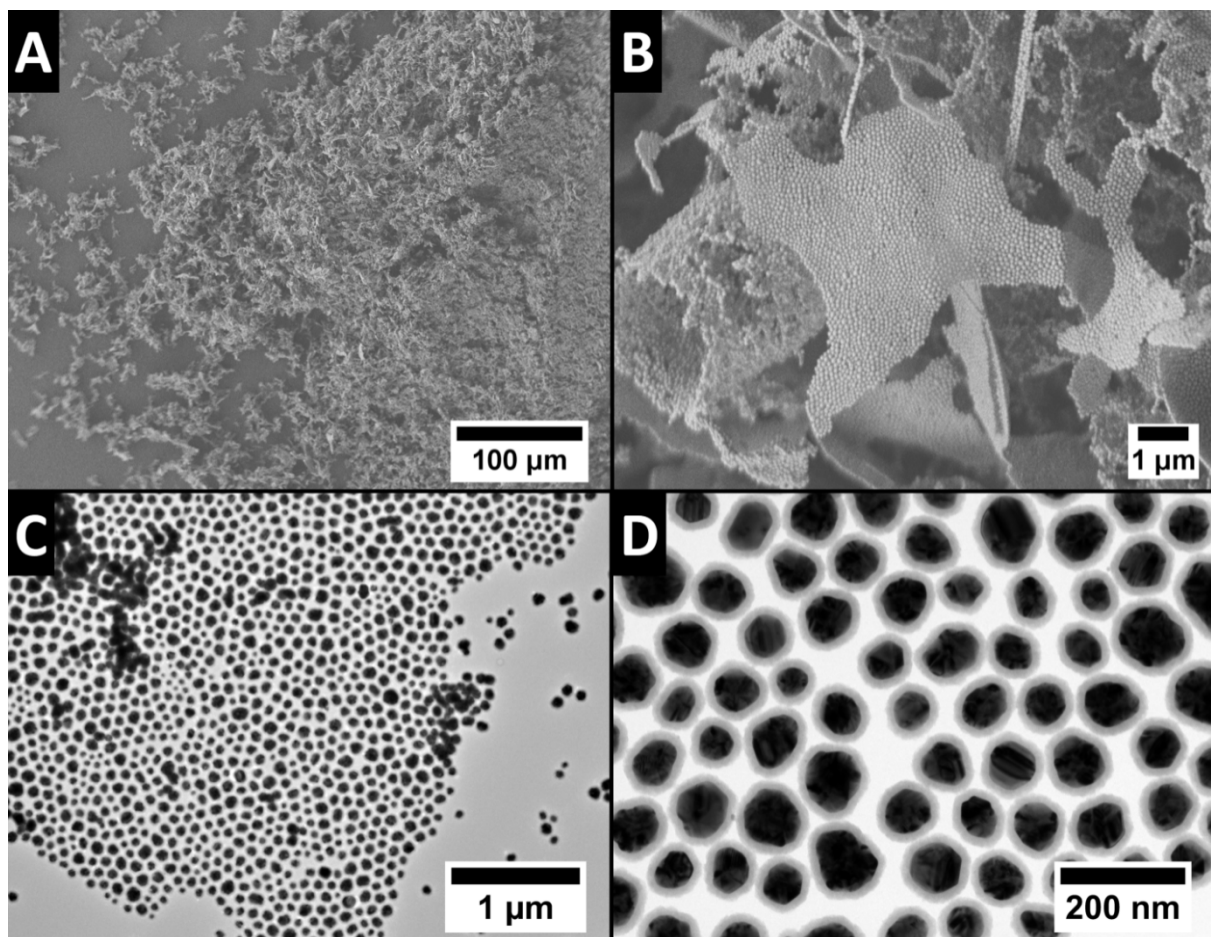


Figure S10. SEM (A+B) and TEM (C+D) characterizations of Ag nanoparticles with a 12 nm silica shell assembled into macroscopic, porous monolithic aerogels. The nanoparticles have interparticle distances of around 25 nm.

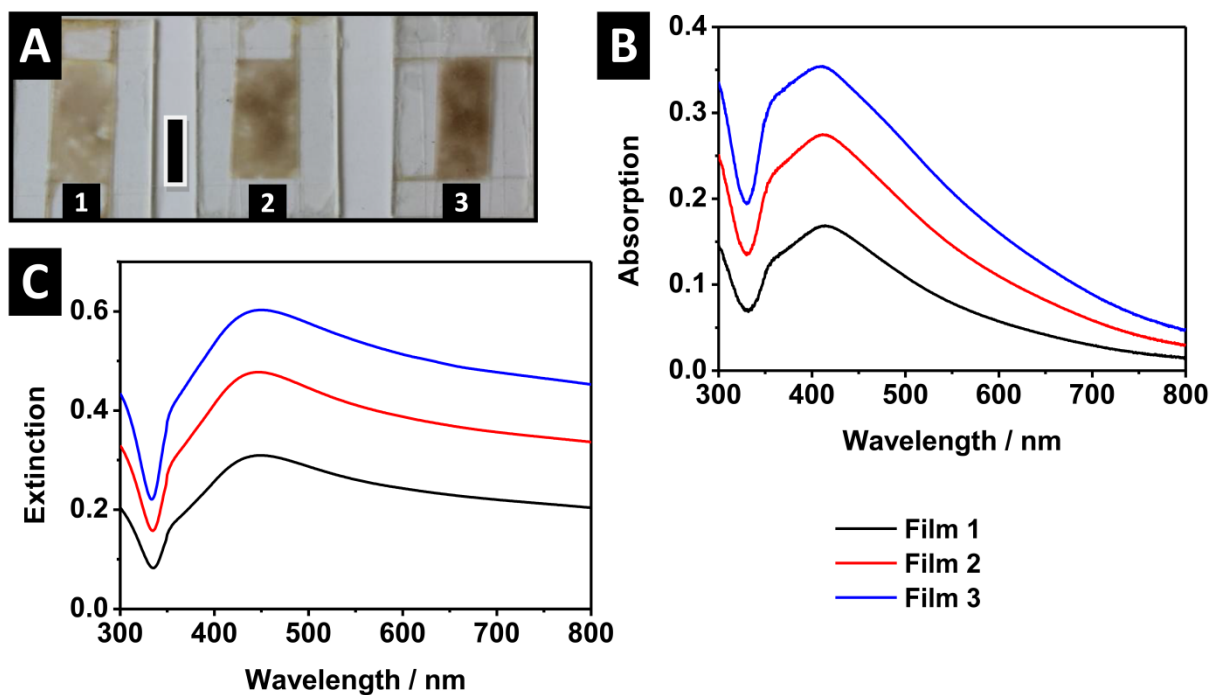


Figure S11. Variation of the Ag-SiO₂ (13 nm silica shell) cryoaerogel film thickness. Photographs (A) of cryoaerogel films with increasing thickness from left (1) to right (3). The black bar represents 1 cm. Absorption (B) and extinction (C) spectra of the respective films show the increase of the optical density with increasing film thickness.

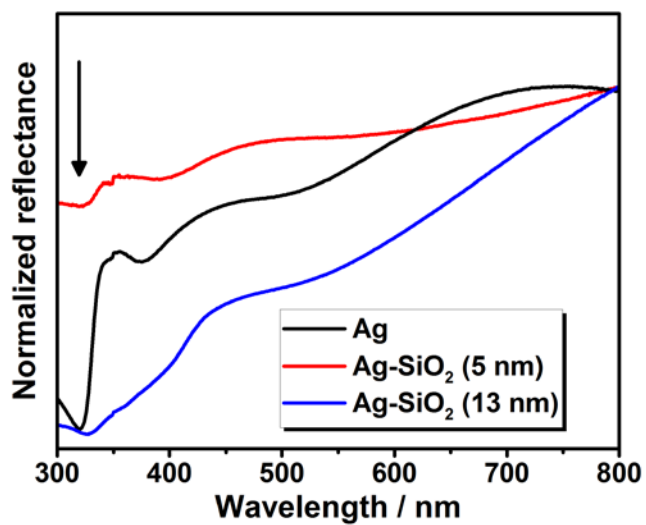


Figure S12. Normalized reflectance spectra of the cryogelated aerogel monoliths. These spectra show the bare Ag (black curve) as well as the Ag-SiO₂ core-shell heterostructures with a shell thickness of 5 nm (red curve) and 13 nm (blue curve). The arrow marks the plasma edge of silver located at around 324 nm.